Analytical Biochemistry **302,** 81–87 (2002)
doi:10.1006/abio.2001.5512, available online at http://www.idealibrary.com on IDEAL®

Probing Reactive Center Loop Insertion in Serpins: A Simple Method for Ovalbumin[1]

Umesh R. Desai,*,[2] Jennifer L. Johns,†,‡ Laura Lahaye,* and H. Tonie Wright†,‡
**Department of Medicinal Chemistry, †Department of Biochemistry, and ‡Institute for Structural Biology and Drug Discovery, Virginia Commonwealth University, Richmond, Virginia 23298*

Received July 19, 2001; published online January 23, 2002

Insertion of the reactive center loop in β-sheet A in serpins has been typically inferred from the increased stability of the cleaved form to thermal- and urea-induced denaturation. We describe a convenient and rapid fluorescence-based method that differentiates the loop-inserted form from the loop-exposed form in ovalbumin, a prototypic noninhibitory serpin. Recombinant wild-type and R345A ovalbumins in the intact form bind ANS with equilibrium dissociation constants of 116 and 125 μM and a maximal fluorescence increase of 200 and 264%, respectively, in pH 6.8 buffer. Cleavage of the two proteins with porcine pancreatic elastase results in a 1.6- and 2.6-fold increase in the ANS-binding affinity. While cleavage of the reactive center loop in rR345A ovalbumin results in a ~200% increase in the ANS fluorescence, the rWT protein exhibits a ~50% decrease. Similar experiments with α_1-proteinase inhibitor and antithrombin, two inhibitory serpins that exhibit reactive center loop insertion, show a decrease in ANS fluorescence on cleavage with porcine pancreatic elastase and thrombin, respectively. Denaturation studies in guanidinium hydrochloride indicate that the reactive center loop is inserted in the main body of the serpin in the cleaved form of rR345A mutant, while it is exposed in the cleaved form of rWT ovalbumin. These results demonstrate that ANS fluorescence change is an indicator of the loop-inserted or loop-exposed form in these recombinant ovalbumins, and thus could be advantageously used for probing reactive center loop insertion in ovalbumins. The major increase in fluorescence for the rR345A mutant on cleavage primarily arises from a change in ANS binding rather than from the generation of an additional ANS-binding site.

The proteins of the serpin (*ser*ine *p*roteinase *in*hibitor) superfamily share a common tertiary structure, which confers unique functional properties that are critical for their roles in numerous physiological processes (1–4). Most serpins are inhibitors of key proteinases involved in these processes, and compromise of their inhibitory activity may lead to a pathological state.

The serpin inhibition mechanism has been investigated in significant detail (2, 3, 5, 6). All known serpins contain a ~15-residue sequence, called the reactive center loop, that recognizes the enzyme's active site. Crystal structures of the intact uncleaved forms of several inhibitory serpins show that the reactive center loop is exposed and is localized at one end of the ellipsoidal body of the serpin, while crystal structures of cleaved inhibitory serpins show the reactive center loop fully inserted into a preexisting β-sheet A (4, 7, 8). This strand insertion is necessary for the formation of the stable serpin-proteinase complex as shown by biochemical studies and the recent crystal structure of such a complex (9, 10). These studies show the proteinase, covalently attached to the P1 residue of the reactive center loop, at the opposite end of the inhibitor, indicating a major translocation of ~70 Å. This occurs in concert with the insertion of the reactive center loop into the main body of the serpin, thereby becoming β-strand 4 of the six-stranded β-sheet A of the inhibitor (4, 7–9). This movement, called the reactive center loop insertion, is characterized by an increase in stability of the loop-inserted form relative to the loop-exposed form under denaturing conditions, such as heat and chaotropic agents. The translocation distorts the catalytic triad of active-site residues of the proteinase, thereby

[1] Supported by research grants from the American Heart Association (U.R.D. and H.T.W.).
[2] To whom correspondence should be addressed at Department of Medicinal Chemistry, P.O. Box 980540, Richmond, VA 23298-0540. Fax: (804) 828-7625. E-mail: urdesai@vcu.edu.

0003-2697/02 $35.00

dramatically reducing the rate of hydrolysis of the acyl-enzyme intermediate resulting in the inhibition of the proteinase (9, 11, 12). Both the thermodynamics and the kinetics of the reactive center loop insertion process are likely to be critical for serpins to successfully inhibit their target proteinases.

Ovalbumin is classified as a serpin based on its three-dimensional structural similarity to the inhibitory serpins (5, 13). Despite this close structural similarity, chicken egg and recombinant wild-type (rWT)[3] ovalbumins are not inhibitors of any serine proteinase (14–16). The reason(s) for the dysfunction of inhibitory mechanism in ovalbumin is(are) not completely understood and is a subject of intense inquiry both to engineer a new inhibitor and to enhance knowledge regarding serpin mechanism. Because ovalbumin is a substrate of elastase (14), and not an inhibitor, the phenomenon of reactive center loop insertion has been commonly inferred in ovalbumin through the attendant increase in stability to thermal- or guanidinium hydrochloride-induced denaturation (16). Both these methods require significant quantities of the protein and are slow and effort intensive. We report here the applicability of measurement of 1-anilinonapthalene-8-sulfonic acid (ANS) fluorescence to deduce reactive center loop insertion in β-sheet A in ovalbumin following cleavage with elastase. The technique is simple, fast, and easy to perform and consumes much less protein than denaturation studies using differential scanning calorimetry, fluorescence, or circular dichroism methods. Preliminary investigations on the interaction of two inhibitory serpins, antithrombin and α_1-proteinase inhibitor, with thrombin and porcine pancreatic elastase, respectively, show that the technique may also be useful for studying reaction kinetics.

MATERIALS AND METHODS

Reagents. 1,8-ANS (99.9%) and guanidinium hydrochloride were purchased from Sigma Chemical Co. (St. Louis, MO). Stock concentration of ANS in 20 mM sodium phosphate buffer, pH 6.8, was prepared using its dry weight. All other chemicals used were reagent-grade Sigma products.

Proteins. Recombinant wild-type and Arg345Ala ovalbumins were overexpressed in bacterial cells from a modified pET3d vector in which the ovalbumin gene was inserted between an introduced *Nsi*I and a *Bam*HI restriction site, essentially as previously described (16). The ovalbumin concentration was calculated from ϵ_{280} of 29,400 M^{-1} cm^{-1} (17). α_1-Proteinase inhibitor (α_1-PI) and porcine pancreatic elastase (PPE) were obtained from either Calbiochem or Sigma and used without further purification. Stock solutions (50–100 μM) of α_1-PI and PPE were prepared in 50 mM Tris-HCl (pH 8.0) and 1 mM HCl, respectively, and stored at −20°C until used. Plasma antithrombin and thrombin were a gift from Professor Steven T. Olson (University of Illinois–Chicago).

Buffer conditions for fluorescence and denaturation studies. Experiments with ovalbumin and antithrombin were performed in a 20 mM sodium phosphate buffer, containing 0.1 mM EDTA, 20 mM NaCl, and 0.1% PEG8000, adjusted to pH 6.8 at 25°C, while a 50 mM Tris-HCl buffer adjusted to pH 8.0 at 25°C was used for α_1-PI experiments. Denaturation studies utilized 8 M guanidinium hydrochloride (GuHCl) in double-distilled deionized water.

Preparation of reactive center loop-cleaved ovalbumins. A ~500 μM recombinant ovalbumin (rWT and rR345A) solution was incubated with 5 μM elastase at 25°C in 100 μL Tris buffer, pH 8.0, for 1 h followed by the addition of 5 μL of 10 mM PMSF. The reaction buffer was immediately exchanged for 20 mM sodium phosphate buffer, pH 6.8, by centrifugal filtration and the cleaved recombinant ovalbumin stored at −20°C until further use. A 10% SDS-PAGE gel showed bands at ~41 kDa (not shown) for both rWTc and rR345Ac ovalbumins confirming reactive center loop cleavage of the intact ovalbumins. Whereas rWTc ovalbumin was homogeneous by SDS-PAGE, the rR345Ac mutant shows two less intense (<2%) fragments at ~30 and ~27 kDa in addition to the major band that possibly arise due to contamination of the porcine pancreatic elastase, as previously reported (14). The presence of these small contaminants in the rR345Ac preparations is not expected to significantly affect the ANS fluorescence results presented here.

Fluorescence and equilibrium-binding studies. The fluorescence emission spectra of ANS in the free and protein-bound state were recorded on a PC1 single-photon-counting fluorescence spectrophotometer (ISS Instruments, Champaign, IL) in ratio mode at ambient temperature. The excitation wavelength was set at 405 nm with a 6-nm bandpass, while the emission was scanned from 450 to 600 nm with a 2-nm bandpass in 1-nm increments. Each spectrum represented an average of 3 scans with a total integration time of 15 s per unit wavelength.

The equilibrium dissociation constants for ANS–recombinant ovalbumin interaction were determined

[3] Abbreviations used: ANS, 1-(anilino)naphthalene-8-sulfonic acid; rWT, recombinant wild-type ovalbumin (recombinant ovalbumin with wild-type sequence); rWTc, porcine pancreatic elastase-cleaved recombinant wild-type ovalbumin; rR345A, recombinant Arg345Ala ovalbumin; rR345Ac, elastase-cleaved Arg345Ala ovalbumin; P14, 14th residue on the N-terminal side of the scissile bond—Schechter and Berger nomenclature (18); α_1-PI, α_1-proteinase inhibitor; PPE, porcine pancreatic elastase; M_T, midpoint of denaturation transition; GuHCl, guanidinium hydrochloride; PEG8000, polyethylene glycol 8000; PMSF, phenylmethylsulfonyl fluoride; SDS-PAGE, sodium dodecyl sulfate-polyacrylamide gel electrophoresis.

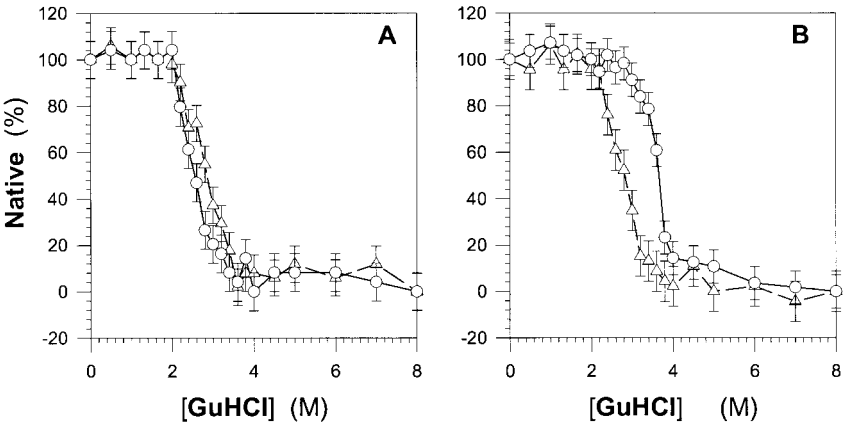

FIG. 1. Guanidinium hydrochloride unfolding profile of intact and cleaved forms of recombinant wild-type (A) and R345A (B) ovalbumins. The triangles (△) represent the intact form while the circles (○) represent the cleaved form in each case. The fraction of molecules in the native conformation was obtained from the change in fluorescence emission maximum as a function of [GuHCl] assuming a linear relationship. Recombinant ovalbumins at 0.5–1 μM in 0–8 M GuHCl were used to obtain the fluorescence spectra (315–365 nm). See text for details.

from the increase in fluorescence intensity at 532 nm (405 nm λ_{EX}) as a function of increasing concentration of the ligand. Titrations were done with ~20 μM solutions of rWT, rR345A, and rWTc ovalbumins and a 5 μM solution of rR345Ac ovalbumin. Simultaneous fluorescence measurements were performed on ANS alone for background subtraction. The increase in fluorescence signal with increasing ANS concentration was fit to the quadratic equilibrium-binding equation, assuming a 1:1 binding stoichiometry.

The interactions of antithrombin and α_1-PI with thrombin and PPE, respectively, were monitored in the presence of 15–30 μM ANS at 25°C. For the antithrombin-thrombin reaction, 20 mM sodium phosphate buffer, pH 7.4, was used whereas 50 mM Tris-HCl buffer, pH 8.0, was used for the α_1-PI–PPE reaction. Fluorescence at 532 nm (λ_{EX} = 405 nm) was averaged every 5 min by integrating the emission intensity for 5 s. Reference fluorescence values of ANS alone and in the presence of the serpin were subtracted for calculating the observed rate constants from the exponential decreases in intensity.

Guanidinium chloride denaturation studies. A ~0.5–1 μM solution of recombinant ovalbumin was incubated in 0–8 M GuHCl for 2 h at room temperature and its fluorescence emission spectrum in the range 315–365 nm (280 nm λ_{EX}) was then recorded using the parameters described above. Emission spectra of GuHCl solutions were recorded under similar conditions and subtracted to obtain the background-corrected emission due to protein. The emission maximum of recombinant ovalbumins changes from ~320 nm in 0 M GuHCl to ~353 nm in 8 M GuHCl. The fraction of protein molecules in the native form was calculated from change in emission maximum as a function of GuHCl concentration.

RESULTS AND DISCUSSION

Recombinant R345A ovalbumin exhibits reactive center loop insertion on cleavage with elastase. Previous work has shown that the replacement of Arg345 (P14 (18)), a critical reactive center loop residue, with Ser confers facile loop insertion on the mutant ovalbumin when cleaved with elastase (16). This observation was also found to be true for an ovalbumin mutant in which the native P12–P10 sequence was mutated to Ala–Ala–Ala in addition to the ArgP14 → Ser replacement. In both these ovalbumins, loop insertion was deduced from the increased stability of the cleaved form of the serpin in comparison to the intact form under denaturing conditions, such as heat or guanidine, as observed for inhibitory serpins (19, 20).

To test whether Ala substitution for this critical P14 residue (R345A ovalbumin) also exhibits the phenomenon of reactive center loop insertion on elastase cleavage, we determined the GuHCl denaturation profiles of the intact and cleaved forms of recombinant wild-type and rR345A ovalbumins (Fig. 1B) (19–23). All four proteins demonstrate a two-state "native ⇔ unfolded" equilibrium transition. While the two-state denaturation transition for the cleaved form of rR345A ovalbumin is similar to that of the cleaved forms of α_1-PI and antithrombin, two prototypic inhibitory serpins, the profiles for the intact forms of recombinant ovalbumins are significantly different from the multistate transitions observed for intact inhibitory serpins (19, 21).

The midpoints of transition (M_T) for the intact forms of rWT and rR345A ovalbumin were observed at 2.8 M GuHCl, while those for the respective cleaved forms (rWTc and rR345Ac) occur at 2.6 and 3.6 M. Thus, whereas the cleavage with elastase reduces the stability of rWT ovalbumin slightly (−0.2 M GuHCl), it in-

creases that of rR345A ovalbumin significantly (+0.8 M GuHCl). This increase in stability of rR345Ac ovalbumin is less than that observed for prototypic inhibitory serpins, including α_1-PI and antithrombin (~2–4 M), following cleavage with their target proteinases (19, 22, 23). However, the transition midpoint for the intact form of recombinant R345A ovalbumin (and of rWT ovalbumin) is found to be 2.8 M, nearly 1 M GuHCl higher than that observed for the intact forms of the inhibitory serpins (1.2–1.8 M GuHCl) (19, 20). Despite this difference, the M_T for the cleaved forms of recombinant ovalbumins studied here and the cleaved forms of the inhibitory serpins are equivalent (~4 M) (19, 22, 23). This indicates that although the increase in stability of rR345A ovalbumin on cleavage is less than that observed for prototypic inhibitory serpins, it is because of the greater stability of the intact form of ovalbumin and not because of the reduced stability of the cleaved form. Thus, the increase in stability of rR345A following elastase cleavage is consistent with the insertion of the reactive center loop in the rR345A mutant but not in rWT ovalbumin. This is further supported by the similarity in the denaturation profiles between rR345Ac ovalbumin and the cleaved forms of α_1-PI and antithrombin.

ANS fluorescence increases significantly on loop insertion. Since Weber and Lawrence's observation of increased fluorescence intensity on binding to serum albumin (24), ANS has been used to investigate conformational and environmental changes in proteins (25–27). The specific advantages of using ANS as a probe of conformational changes are its propensity to bind most proteins, an increase in its quantum yield in the protein-bound state, and the kinetic characteristics of interaction. Its relatively weak binding affinity, arising from a high off rate (100–1000 s^{-1}) and a high on rate (~10^8 M^{-1} s^{-1}), suggests that the kinetics of ANS association and dissociation would not limit the process under observation (28).

Previous studies on the chicken egg ovalbumin–ANS interaction suggest that the weak binding is accompanied by a small increase in fluorescence (29, 30) that could be difficult to follow. To investigate whether recombinant ovalbumins that lack the glycosyl chains differ from the wild type, we measured the fluorescence emission spectra of ANS in the presence of these different forms. The ANS emission spectra showed a characteristic increase in fluorescence intensity due to protein binding for the ovalbumin mutants studied here (rWT, rWTc, rR345A, and rR345Ac), as expected. Excitation of ANS at 405 nm led to "double-humped" emission spectra with maximal intensities at 494 and 532 nm (intensity ratio of ~1:1.5–1:2, respectively) for complexes with all four ovalbumins at pH 6.8 (not shown). Similar double-humped fluorescence spectra have been observed for egg ovalbumin and thyroxine-binding globulin, a noninhibitory serpin (31). Although the interaction of ANS with recombinant ovalbumins could be successfully monitored at both wavelengths, we monitored all the subsequent experiments at 532 nm due to the higher sensitivity at this wavelength.

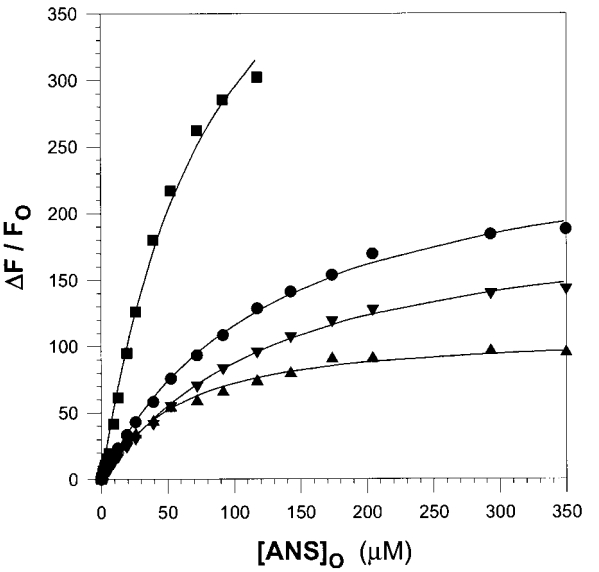

FIG. 2. Differential increase in fluorescence of ANS on interacting with rWT (▼), rWTc (▲), rR345A (●), and rR345Ac (■) ovalbumins. Shown is the background-subtracted increase in fluorescence intensity at 532 nm (λ_{EX} = 405 nm) by sequential addition of ANS at fixed serpin concentrations (5–20 μM) in 20 mM sodium phosphate buffer, pH 6.8. The increase in fluorescence at saturation was used to determine the equilibrium dissociation constant of interaction assuming a 1:1 binding stoichiometry (26).

Figure 2 shows the fluorescence intensity profiles of ANS binding to the intact and cleaved forms of rWT and rR345A ovalbumins. The fluorescence increases as a function of ANS concentration for all four proteins, suggesting the formation of ANS–serpin complexes. However, the magnitude of this increase in fluorescence varies among the four ovalbumins, most dramatically for the cleaved form of rR345A ovalbumin. Thus, whereas the maximal fluorescence intensity increase is 200, 109, and 264% for rWT, rWTc, and rR345A ovalbumins, respectively, the cleaved form of rR345A (rR345Ac) shows a 535% increase at saturation (Table 1). Thus, the fluorescence increases ~2-fold for rR345A ovalbumin following elastase cleavage, while it decreases ~50% for recombinant wild-type ovalbumin. In concert with the results described above using GuHCl denaturation studies, these characteristic differences suggest that ANS fluorescence could be used to distinguish the loop-inserted and loop-exposed forms in ovalbumins. Thus, ANS-based fluorescence assay can conveniently probe the insertion of reactive center loop in ovalbumins.

TABLE 1

Equilibrium Dissociation Constant (K_D), Maximal Fluorescence Change (ΔF_{MAX}), and Denaturation Midpoint of Transition (M_T) for ANS–Recombinant Ovalbumin Interaction

	ΔF_{MAX} %	K_D μM	M_T (M GuHCl)
rWT	200 ± 8	116 ± 10	2.8 ± 0.2
rWTc	109 ± 6	44 ± 8	2.6 ± 0.2
rR345A	264 ± 10	125 ± 10	2.8 ± 0.2
rR345Ac	535 ± 70	78 ± 20	3.6 ± 0.2

Note. The K_D and ΔF_{MAX} were determined from the increase in ANS fluorescence following interaction with the serpin at 25°C in 20 mM sodium phosphate buffer at pH 6.8 at ambient temperature assuming a 1:1 binding stoichiometry. The M_T (in [GuHCl]) was determined from the change in emission maximum that follows denaturation with sequential addition of guanidinium hydrochloride. Error shown represents ±2 SE. See Materials and Methods.

The increase in fluorescence plateaus at sufficiently high ANS concentrations to afford a convenient method of obtaining the equilibrium dissociation constant. Assuming a binding stoichiometry of 1:1, as deduced for the chicken egg ovalbumin–ANS interaction (29), K_D values of 116, 44, 125, and 78 μM were obtained for the rWT, rWTc, rR345A, and rR345Ac ovalbumin, respectively (Table 1). These values indicate that ANS-binding affinity increases 2.6- and 1.6-fold for the rWT and rR345A proteins, respectively, on elastase cleavage of the reactive center loop.

To determine whether loop insertion in other related serpins is also accompanied by a change in ANS fluorescence, we investigated antithrombin and α_1-PI, both of which exhibit loop insertion in inhibiting their target enzymes (1–3). The interaction of antithrombin and α_1-PI with their target proteinases, thrombin and PPE, respectively, was monitored under pseudo-first-order conditions as a function of time using ANS fluorescence emission at 532 nm (Fig. 3). The fluorescence decreases exponentially for both systems with second-order rate constants of 1.1×10^4 and 8.0×10^5 M^{-1} s^{-1} for antithrombin–thrombin and α_1-PI–PPE, respectively. These correspond favorably with the second-order inhibition rate constants (9×10^3 and 5×10^5, respectively) measured for the two systems using extensive enzyme inhibition assays (32, 33). Recently the interaction of plasminogen activator inhibitor-1 with urokinase-type plasminogen activator was shown to result in ~70% decrease (34), while α_1-antitrypsin–rat trypsin interaction led to a 50% increase in ANS fluorescence (20). Thus, the phenomenon of loop insertion can be rapidly assessed using the significant differences in ANS-binding properties of the loop-inserted and -exposed forms of several serpins.

To probe in more detail whether the dramatic fluorescence change observed on elastase cleavage of rR345Ac arises from a reorganization of the ANS-binding site or from the generation of an additional binding site(s) following loop insertion, the fluorescence change was monitored as a function of increasing rR345Ac concentration (Fig. 4A). Extrapolating the fluorescence increase to infinite protein concentration at which all ANS is bound permits the determination of the change in fluorescence per mole of ANS bound. This calibration value was then used to determine the fraction of bound ANS by titrating rR345Ac with ANS (Fig. 4B), as previously described (29). The resultant fluorescence change could be analyzed using the Klotz relationship (Eq. [1]) that describes interactions of low-molecular-weight dyes with proteins (35).

$$\frac{[\text{rR345Ac}]}{[\text{ANS}]}\frac{1}{f_x} = \frac{1}{n}\left(1 + \frac{K_D}{(1-f_x)}\frac{1}{[\text{ANS}]}\right) \qquad [1]$$

where f_x is the fraction of ANS bound, K_D is the equilibrium dissociation constant of interaction, and n is the binding stoichiometry.

Fitting the data in Fig. 4B to the above relationship gives a K_D of 39 ± 27 μM. This value is similar to that determined by direct titration (78 ± 20 μM). A stoichiometry (n) of 0.8 ± 0.4 is observed for the rR345Ac–ANS interaction, suggesting that reactive center loop cleavage does not generate an additional binding site in the cleaved form of this mutant. Thus, it is likely

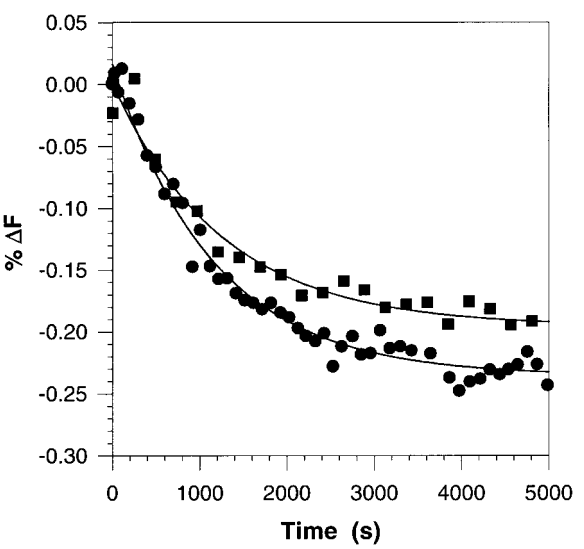

FIG. 3. Fluorescence of the bound ANS on interaction of antithrombin (●) and α_1-PI (■) with thrombin and PPE, respectively. The emission intensity at 532 nm was followed as a function of time following the addition of the enzyme (~50–100 nM) to the serpin (~0.5–1 μM) in pH 7.4 or 8.0 buffer at 25°C. The solid line represents an exponential fit to the data to derive the observed rate constant of the reaction. The observed decrease (~20%) in fluorescence is a fraction of the total decrease expected at the end of the reaction (~60–80%) due to pseudo-first-order conditions employed in the experiments.

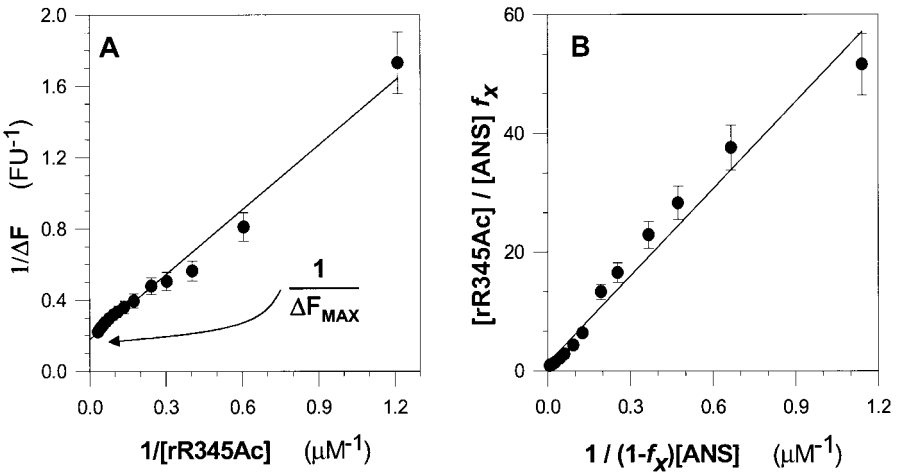

FIG. 4. Stoichiometry of binding for rR345Ac–ANS interaction. The reciprocal of increase in fluorescence on titrating 5 μM ANS solution with rR345Ac was extrapolated to infinite serpin concentration (the intercept of abscissa = $1/\Delta F_{MAX}$) to deduce the fluorescence change per mole of ANS bound (ΔF/[bound ANS]) under standardized conditions (A). This value was used to determine the fraction of bound ANS (f_x = [bound ANS]/$[ANS]_O$) in a titration at fixed [rR345A] concentration. The resultant data (B) were fit to the Klotz equation (Eq. [1]) to obtain the K_D of interaction and stoichiometry of binding (n). The conditions used for these experiments were identical to those for the fluorescence titrations described above. See text for details.

that a reorganization or change in accessibility of an ANS-binding site, already present in intact rR345A ovalbumin, occurs following reactive center loop insertion, which dramatically enhances the ANS quantum yield in the cleaved form.

In conclusion, the measurement of ANS fluorescence changes following reactive center loop cleavage of recombinant ovalbumin is a convenient technique for deducing loop insertion in β-sheet A. This is a simple, rapid assay consuming much smaller amounts of the protein than typical extensive denaturation studies. In addition, the kinetics of the loop insertion process may be determined using the time dependence of the ANS fluorescence signal.

REFERENCES

1. Stein, P. E., and Carrell, R. W. (1995) What do dysfunctional serpins tell us about molecular mobility and disease? *Nature Struct. Biol.* **2,** 96–113.
2. Potempa, J., Korzus, E., and Travis, J. (1994) The serpin superfamily of proteinase inhibitors: Structure, function, and regulation. *J. Biol. Chem.* **269,** 15957–15960.
3. Gettins, P. G., Patston, P. A., and Olson, S. T. (1996) Serpins: Structure, Function and Biology, pp. 33–63, Landes, Austin, TX.
4. Whisstock, J., Skinner, R., and Lesk, A. M. (1998) An atlas of serpin conformations. *Trends Biochem. Sci.* **23,** 63–67.
5. Wright, H. T. (1996) The structural puzzle of how serpin serine proteinase inhibitors work. *BioEssays* **18,** 453–464.
6. Wright, H. T., and Scarsdale, J. N. (1995) Structural basis of serpin inhibitor activity. *Proteins: Struct., Funct. Genet.* **22,** 210–225.
7. Whisstock, J., Skinner, R., Carrell, R., and Lesk, A. (2000) Conformational changes in serpins: I. Native and cleaved conformations of α1-antitrypsin. *J. Mol. Biol.* **295,** 651–665.
8. Schreuder, H. A., de Boer, B., Dijkema, R., Mulders, J., Theunissen, H. J. M., Grootenhuis, P. D. J., and Hol, W. G. J. (1994) The intact and cleaved human antithrombin III complex as a model for serpin-proteinase interactions. *Nature Struct. Biol.* **1,** 48–54.
9. Huntington, J. A., Read, R. J., and Carrell, R. W. (2000) Structure of a serpin-protease complex shows inhibition by deformation. *Nature* **407,** 923–926.
10. Stratikos, E., and Gettins, P. (1999) Formation of the covalent serpin-proteinase complex involves translocation of the proteinase by more than 70 Å and full insertion of the reactive center loop into beta-sheet A. *Proc. Natl. Acad. Sci. USA* **96,** 4808–4813.
11. Plotnick, M. I., Mayne, L., Schechter, N. M., and Rubin, H. (1996) Distortion of the active site of chymotrypsin complexed with a serpin. *Biochemistry* **35,** 7586–7590.
12. Calugaru, S. V., Swanson, R., and Olson, S. T. (2001) The pH dependence of serpin-proteinase complex dissociation reveals a mechanism of complex stabilization involving inactive and active conformational states of the proteinase which are perturbable by calcium. *J. Biol. Chem.* **276,** 32446–32455.
13. Gettins, P. G. W., Patston, P. A., and Schapira, M. (1993) The role of conformational change in serpin structure and function. *BioEssays* **15,** 461–467.
14. Wright, H. T. (1984) Ovalbumin is an elastase substrate. *J. Biol. Chem.* **259,** 14335–14336.
15. Wright, H. T., Qian, H. X., and Huber, R. (1990) Crystal structure of plakalbumin, a proteolytically nicked form of ovalbumin. Its relationship to the structure of cleaved alpha-1-proteinase inhibitor. *J. Mol. Biol.* **213,** 513–528.
16. Huntington, J. A., Fan, B., Karlsson, K. E., Deinum, J., Lawrence, D. A., and Gettins, P. G. W. (1997) Serpin conformational change in ovalbumin. Enhanced reactive center loop insertion through hinge region mutations. *Biochemistry* **36,** 5432–5440.
17. Joniau, M., Bloemmen, J., and Lontie, R. (1972) The reaction of 4-(p-sulfophenylazo)-2-mercuriphenol with the thiol groups of proteins. *Biochim. Biophys. Acta* **214,** 468–477.

18. Schechter, I., and Berger, A. (1967) On the size of the active site in proteases: I: Papain. *Biochem. Biophys. Res. Commun.* **27,** 157–162.
19. Bruch, M., Weiss, V., and Engel, J. (1988) Plasma serine proteinase inhibitors (serpins) exhibit major conformational changes and a large increase in conformational stability upon cleavage at their reactive sites. *J. Biol. Chem.* **263,** 16626–16630.
20. Kaslik, G., Kardos, J., Szabo, E., Szilagyi, L., Zavodszky, P., Westler, W. M., Markley, J. L., and Graf, L. (1997) Effects of serpin binding on the target proteinase: Global stabilization, localized increased structural flexibility, and conserved hydrogen bonding at the active site. *Biochemistry* **36,** 5455–5464.
21. Powell, L. M., and Pain, R. H. (1992) Effects of glycosylation on the folding and stability of human, recombinant and cleaved alpha 1-antitrypsin. *J. Mol. Biol.* **224,** 241–252.
22. Lukacs, C. M., Zhong, J. Q., Plotnick, M. I., Rubin, H., Cooperman, B. S., and Christianson, D. W. (1996) Arginine substitutions in the hinge region of antichymotrypsin affect serpin beta-sheet rearrangement. *Nature Struct. Biol.* **3,** 888–893.
23. Lee, K. N., Im, H., Kang, S. W., and Yu, M.-H. (1998) Characterization of a human alpha1-antitrypsin variant that is as stable as ovalbumin. *J. Biol. Chem.* **273,** 2509–2516.
24. Weber, G., and Lawrence, D. J. R. (1954) Fluorescent indicators of adsorption in aqueous solution and on the solid phase. *Biochem. J.* **56,** xxxi.
25. Masui, R., and Kuramitsu, S. (1998) Probing of DNA-binding sites of Escherichia coli RecA protein utilizing 1-anilinonaphthalene-8-sulfonic acid. *Biochemistry* **37,** 12133–12143.
26. Kirk, W. R., Kurian, E., and Prendergast, F. G. (1996) Characterization of the sources of protein-ligand affinity: 1-Sulfonato-8-(1′)anilinonaphthalene binding to intestinal fatty acid binding protein. *Biophys. J.* **70,** 69–83.
27. Berggard, T., Silow, M., Thulin, E., and Linse, S. (2000) Ca(2+)- and H(+)-dependent conformational changes of calbindin D(28k). *Biochemistry* **39,** 6864–6873.
28. Regenfuss, P., and Clegg, R. (1987) Diffusion-controlled association of a dye, 1-anilinonaphthalene-8-sulfonic acid, to a protein, bovine serum albumin, using a fast-flow microsecond mixer and stopped-flow. *Biophys. Chem.* **26,** 83–89.
29. Cardamone, M., and Puri, N. K. (1992) Spectrofluorimetric assessment of the surface hydrophobicity of proteins. *Biochem. J.* **282,** 589–593.
30. Chang, L. S., Wen, E. Y., Hung, J. J., and Chang, C. C. (1994) Energy transfer from tryptophan residues of proteins to 8-anilinonaphthalene-1-sulfonate. *J. Protein Chem.* **13,** 635–640.
31. Green, I. M., Marshall, J. S., Pensky, J., and Stanbury, J. B. (1972) Studies on human thyroxine-binding globulin. VII. The effect of environmental changes on the fluorescence of I,8-anilinonaphthalene sulfonic acid bound to thyroxine-binding globulin. *Biochim. Biophys. Acta* **278,** 305–315.
32. Olson, S. T., Bjork, I., and Shore, J. D. (1993) Kinetic characterization of heparin-catalyzed and uncatalyzed inhibition of blood coagulation proteinases by antithrombin. *Methods Enzymol.* **222,** 525–559.
33. Laurent, P., and Bieth, J. G. (1989) Kinetics of the inhibition of free and elastin-bound human pancreatic elastase by alpha 1-proteinase inhibitor and alpha 2-macroglobulin. *Biochim. Biophys. Acta* **994,** 285–288.
34. Egelund, R., Einholm, A. P., Pedersen, K. E., Nielsen, R. W., Christensen, A., Deinum, J., and Andreasen, P. A. (2001) A regulatory hydrophobic area in the flexible joint region of plasminogen activator inhibitor-1, defined with fluorescent activity-neutralizing ligands. Ligand-induced serpin polymerization. *J. Biol. Chem.* **276,** 13077–13086.
35. Klotz, I. (1947) The effects of salts and proteins on the spectra of some dyes and indicators. *Chem. Rev.* **41,** 373–399.